A STUDY OF SUPERNOVA REMNANTS WITH CENTER-FILLED X-RAY MORPHOLOGY

NASA Grant NAG5-3486

Annual Report

For the Period 15 November 1996 through 14 November 1997

Principal Investigator
Dr. Patrick O. Slane

September 1997

Prepared for:

National Aeronautics and Space Administration
Goddard Space Flight Center
Greenbelt, Maryland 20771

Smithsonian Institution
Astrophysical Observatory
Cambridge, Massachusetts 02138

The Smithsonian Astrophysical Observatory
is a member of the
Harvard-Smithsonian Center for Astrophysics

The NASA Technical Officer for this grant is Donald K. West, 681.0, National Aeronautics **and Space Administration, G**oddard Space Flight Center, Greenbelt, Maryland 20771.

The subject grant is for work on a project entitled "A Study of Supernova Remnants With Center-Filled X-Ray Morphology." The proposed study entails use of archival data, primarily from past and active X-ray observatories, to study the properties of a class of supernova remnants (SNRs) which display a centrally-bright X-ray morphology. Several models which have been proposed to explain the morphology are being investigated for comparisons with measured characteristics of several remnants: nonthermal emission from a central synchrotron nebula; thermal emission enhanced by slow evaporation of cool clouds in the hot SNR interior; and relic thermal emission from the SNR interior after the remnant has entered the radiative phase of evolution, thus causing the shell emission to cease.

In the first year of this study, we have investigated the X-ray emission properties of five SNRs. Below we summarize the results for each:

The remnant 3C58 is a known nonthermal source. The centrally bright morphology is the result of a synchrotron nebula which is powered by an as-yet unidentified pulsar. In our study of 3C58, using data obtained from the ASCA Observatory, we were able to show for the first time that the spectral index varies with radius as expected from synchrotron lifetime constraints. In addition, we established stringent limits on the presence of any thermal emission component associated with the SNR blast wave. A paper on this work entitled "ASCA Observations of the Crab-like Supernova Remnant 3C58" (by Torii, Kinugasa, Hashimotodani, Tsunemi, & Slane) has been submitted for publication in *Publications of the Astronomical Society of Japan.*

We have also studied the emission from the centrally-bright remnant CTA 1. Our earlier work on this remnant showed that the ROSAT PSPC data were unable to distinguish between thermal and nonthermal spectral models for the emission. We thus carried out observations of the central region with ASCA. We find that the central spectrum is clearly nonthermal, suggesting the presence of a central pulsar. Properties of a faint central point source observed with ROSAT are consistent with those expected for the pulsar. The results have been summarized in a paper entitled "Nonthermal X-ray Emission from CTA 1" (Slane *et al.* 1997). A copy of the paper is attached.

MSH 11-62 is a centrally-bright SNR whose radio morphology is sug-

gestive of a composite SNR whose central emission is powered by a pulsar, similar to what we have determined for CTA 1. Our ASCA observations confirm this scenario and allow us to model both the synchrotron component and the blast wave component. Results from this study were presented at the Minnesota Astronomy Centennial workshop; a copy of the abstract is attached. A paper entitled "A Study of the Composite Remnant MSH 11-62" (by Harrus, Hughes, & Slane) has been submitted to *The Astrophysical Journal.*"

Spectra from MSH 11-61A and W28 reveal that the emission is clearly thermal in nature for both sources. Comparisons of the spectral and morphological characteristics with models for SNR evolution in a cloudy interstellar medium (ISM) and for models of radiative-phase remnants are in progress. Results for MSH 11-61A, and preliminary results for W28, were presented at the Minnesota Astronomy Centennial workshop; a copy of the abstract is attached. A paper summarizing the results for MSH 11-61A is in preparation.

THE ASTROPHYSICAL JOURNAL, 485:221–227, 1997 August 10

NONTHERMAL X-RAY EMISSION FROM CTA 1

PATRICK SLANE,[1] FREDERICK D. SEWARD,[1] RINO BANDIERA,[2] KEN'ICHI TORII,[3] AND HIROSHI TSUNEMI[3,4]
Received 1996 December 19; accepted 1997 March 3

ABSTRACT

CTA 1 is a center-filled supernova remnant (SNR) whose morphology and spectrum indicate the presence of a central pulsar, a synchrotron nebula, and a thermal component associated with the expansion of the blast wave into the interstellar medium. The centrally bright emission surrounds the position of a faint point source of X-rays observed with the *ROSAT* PSPC. Here we report on *ASCA* observations that confirm the nonthermal nature of the diffuse emission from the central regions of the remnant. We also present evidence for weak thermal emission that appears to increase in strength toward the outer boundary of the SNR. Thus, CTA 1 appears to be an X-ray composite remnant. Both the aftermath of the explosive supernova event and the energetic compact core are observable.

Subject headings: ISM: individual (CTA 1) — supernova remnants — X-rays: ISM

1. INTRODUCTION

An important class of supernova remnants (SNRs) is characterized by centrally bright X-ray emission accompanied by a radio shell. In several cases (e.g., W49B [Smith et al. 1985]; W44 [Rho et al. 1994; Harrus et al. 1997]) the X-ray emission is clearly thermal in nature. Our *ROSAT* studies of CTA 1 (Seward, Schmidt, & Slane 1995, hereafter SSS95) suggest a different scenario for this remnant. The central emission is dominated by a power-law component, probably driven by an as yet undiscovered pulsar, while the outer regions are dominated by a thermal component associated with the SNR blast wave. In this paper we present results from new X-ray observations of CTA 1, carried out with the *Advanced Satellite for Cosmology and Astrophysics* (*ASCA*) observatory, that confirm the nonthermal nature of the central emission as well as the presence of a weak soft component which we attribute to thermal emission from the shock-heated swept-up interstellar medium (ISM).

Our initial studies of CTA 1 (SSS95) incorporated three ~10 ks Position Sensitive Proportional Counter (PSPC) observations to map the ~100′ remnant (Fig. 1). A 3 ks HRI observation was used to determine an accurate position for the brightest source in the remnant image (1E 0000+726 which has been subtracted from Fig. 1). Optical observations identified the source as a background active galactic nucleus (AGN); the position of this source is indicated in Figure 1.

The spatial distribution of the X-ray emission, which peaks in the central regions, extends out to the radio shell (Fig. 2); the X-ray rim is sharpest in the south, where the radio shell is brightest (Pineault et al. 1993). A faint point source ($R_{\rm PSPC} = 4.5 \times 10^{-3}$ counts s^{-1}) resides within the bright central region, where the count rate is 0.32 counts s^{-1} averaged over a circle of 10′ radius. A ridge of radio emission extends from the south toward the center of the remnant, but there is no clear evidence of a radio plerion at the position of the X-ray central source. The southern boundary of the X-ray emission coincides with the bright radio shell, and a ridge of emission similar to that seen in the radio image extends back to the bright center. The X-ray emission extends beyond the radio in the northern portions of CTA 1 where the radio shell is incomplete, perhaps suggestive of a blowout into a preexisting cavity (Pineault et al. 1993); recent radio images at higher sensitivity (Pineault et al. 1997) reveal faint radio emission from this region of extended X-ray emission as well.

Spectral studies with the PSPC show clearly that a simple one-temperature thermal spectrum (Raymond & Smith 1977) is not compatible with the data—a result which is not surprising for emission from an SNR. Addition of a power-law component provides an acceptable fit to the data, as does addition of a second, higher temperature, thermal component. The PSPC data cannot discriminate between the two models. However, based upon modeling efforts in which we attempted to reproduce the centrally bright morphology of the remnant (SSS95), we concluded that the temperature profile implied by the thermal model was difficult to reproduce. A plausible alternative interpretation was that CTA 1 is described by a central power law (probably associated with a pulsar) combined with a thermal component which we attribute to the SNR shock.

Spectra extracted from several discrete regions of the remnant show that the power-law component becomes weaker farther from the center of the remnant, consistent with the interpretation of a central plerion (Fig. 3); the power-law component comprises ~90% of the 0.1–2.4 keV flux in the central regions, while the outer regions are dominated by a ~50%–80% thermal component. The PSPC data show some evidence of a softening of the power-law spectrum with radius as well. *ASCA* studies of the Crab-like remnant 3C 58 reveal similar results (Torii et al. 1996).

2. *ASCA* OBSERVATION

The central region of CTA 1 was observed with *ASCA* for 40 ks on 1996 January 25. To increase the available time resolution for the GIS data, some telemetry bits from the pulse-height analyzer (PHA) and rise-time data were sacrificed. The resulting 256 PHA channels do not degrade the spectral resolution beyond that inherent to the GIS. However, all rise-time information was sacrificed for data taken with medium bit rate. Such loss of rise-time data does

[1] Harvard-Smithsonian Center for Astrophysics, 60 Garden Street, Cambridge, MA 02138.
[2] Osservatorio Astrofisico di Arcetri, Largo E Fermi 5, 50125 Firenze, Italy.
[3] Department of Earth and Space Science, Osaka University 1-1, Machikaneyama-cho, Toyonaka, Osaka, 560, Japan.
[4] CREST, Japan Science and Technology Corporation (JST).

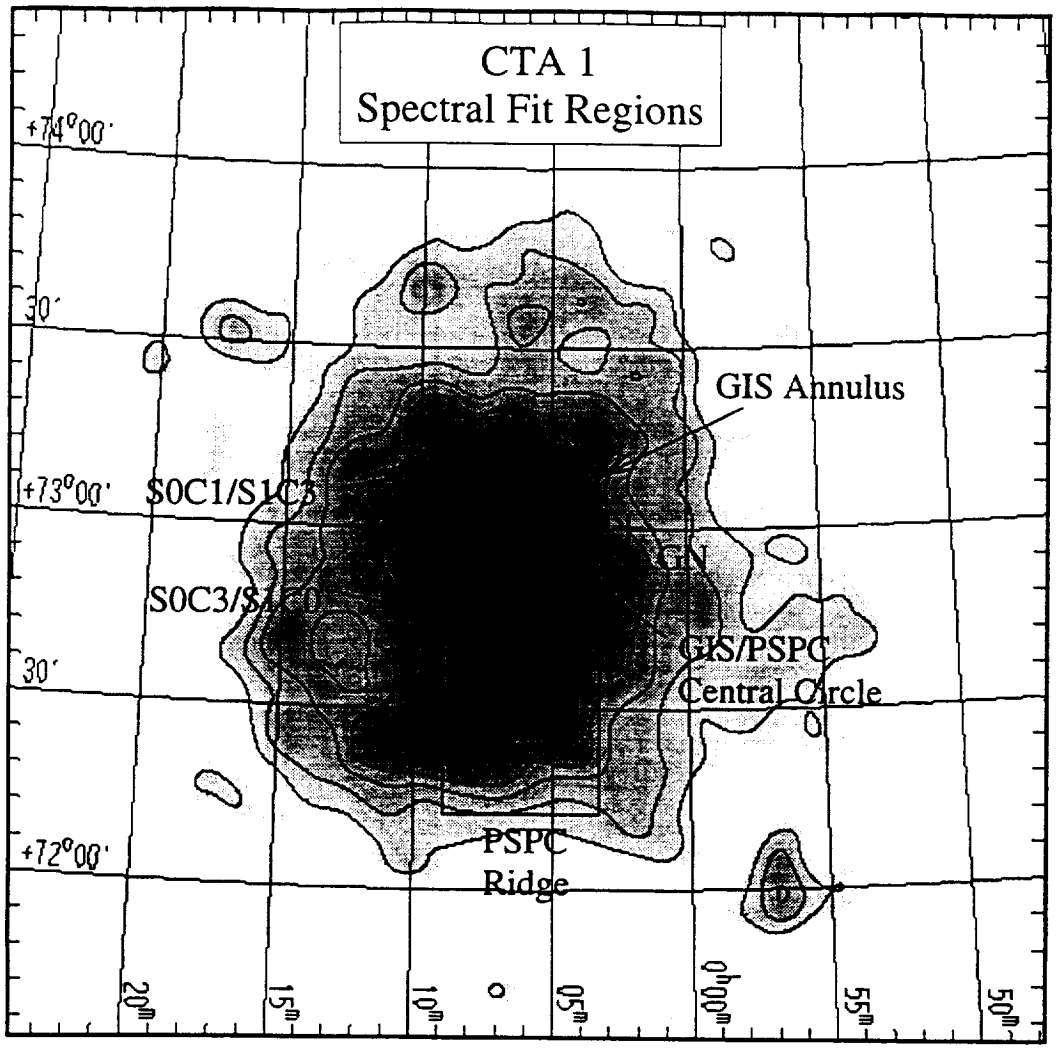

FIG. 1.—PSPC image of CTA 1. Spectral results are consistent with a power law that is strongest at the bright central region, in combination with a soft thermal component that may be associated with shocked ISM. The grid is in J2000 coordinates. Spectral fitting fields are indicated schematically: the inner circle corresponds to central GIS and PSPC fields; the outer annulus corresponds to the outer GIS field; SIS fields are as indicated; PSPC ridge refers to one discrete region used in SSS95 and illustrated in Fig. 3. The location of the AGN which has been subtracted from image is indicated with a plus sign.

slightly compromise the ability to reject background, but the resulting effect on spectral characterization is not large. The approach then provides time resolution of ~4 ms for medium bit rate telemetry data and ~15 ms for high bit rate data. This resolution is crucial to a search for high-frequency pulsations which might arise from a central pulsar.

After screening to remove data taken at low magnetic rigidity or small Earth angle, we obtained a total of ~20,000 events (~41 ks) from each GIS detector (~57% of which was in high bit rate mode). The SIS data were acquired in 2 CCD mode because of the reduced spectral resolution and increased problems with flickering pixels associated with 4 CCD mode. Chips S0C1 and S1C3 covered the region centered on the peak X-ray brightness, while chips S0C3 and S1C1 covered the region directly south of the center (Fig. 1). After screening and removal of flickering pixels, we obtained a total of ~12,000 events from each SIS detector (approximately 7500 of which were from the chip covering the bright central region).

3. ANALYSIS

3.1. *Spectral*

Our investigation included separate analysis of the GIS and SIS data as well as joint fits using the GIS, SIS, and PSPC data. Background for the *ASCA* data was obtained from blank-sky observations available in the *ASCA* data archive. While these were carried out at high Galactic latitude, they provide an adequate description of the background for CTA 1, which has a Galactic latitude of 10°.5; the background-subtracted spectra show no signs of a hard thermal component with line features which might be expected from Galactic ridge emission at lower latitudes (Yamauchi et al. 1996). The GIS and SIS data both reveal featureless spectra consistent with a power law of photon index $\alpha \sim 2$. In each case, addition of a small thermal component at $kT \sim 0.2$ keV yields a statistically significant improvement in the fit.

For more detailed analysis, we extracted GIS2, GIS3, and PSPC spectra from circular regions of radius 9'.2 centered

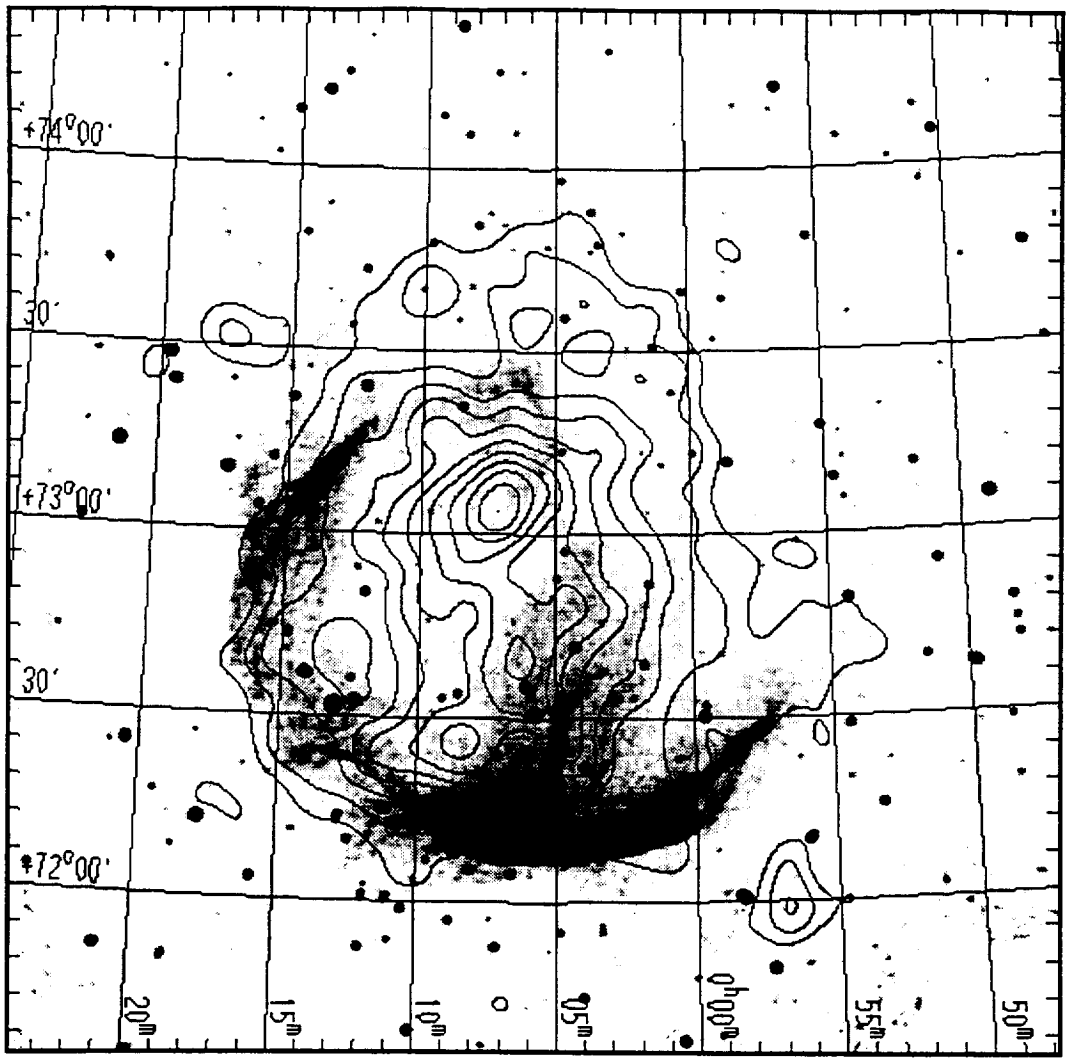

FIG. 2.—Continuum emission from CTA 1 at 1420 MHz (Pineault et al. 1993). X-ray contours correspond to the *ROSAT* PSPC image. The southern edge of the X-ray emission corresponds well with the bright radio shell. Similarly, there is evidence in the radio for a bridgelike structure extending toward the center, similar to that seen in X-rays. The most recent radio maps (Pineault et al. 1996) show faint radio emission extending to the outer X-ray contours in the north and northwest.

on the bright central region. We performed joint fits on these data along with SIS data from chips S0C1 and S1C3. The inclusion of the PSPC data was particularly important in helping to constrain the value of N_H. Normalizations for each detector were varied independently to allow for differences in field of view and point-spread function. The fit to a composite thermal/nonthermal spectrum yields a reduced χ^2 of 1.17 for the best-fit parameters given in Table 1.

We next searched for evidence of spectral variations across the remnant. Here we fixed the column density at the best-fit value derived above. Using the SIS chip centered on the bright central region, the measured photon index is $\alpha = 2.1 \pm 0.1$ (Fig. 4), the same within the small uncertainty as that for the Crab Nebula. The power-law fit is sta-

TABLE 1

CTA 1 SPECTRAL PARAMETERS

Region	Data	Parameter	Value
Central 9'.2	GIS, SIS, and PSPC	N_H	$2.8^{+0.6}_{-0.5} \times 10^{21}$ cm^{-2}
Central 9'.2	GIS, SIS, and PSPC	α (photon)	$2.03^{+0.05}_{-0.07}$
Central 9'.2	GIS, SIS, and PSPC	kT	0.21 ± 0.03 keV
$0 < R < 9'.2$	GIS	F_X (thermal)	2.7×10^{-12} ergs cm^{-2} s^{-1}
$0 < R < 9'.2$	GIS	F_X (nonthermal)	9.5×10^{-12} ergs cm^{-2} s^{-1}
$9'.2 < R < 18'.5$	GIS	F_X (thermal)	1.3×10^{-11} ergs cm^{-2} s^{-1}
$9'.2 < R < 18'.5$	GIS	F_X (nonthermal)	1.4×10^{-11} ergs cm^{-2} s^{-1}

NOTE.—All fluxes are 0.5–10 keV.

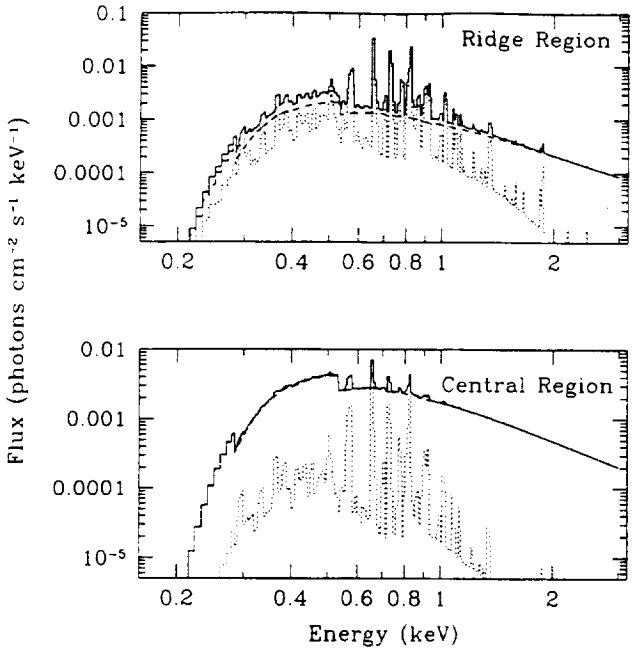

FIG. 3.—Best-fit spectral components and their sum for power-law plus thermal model to PSPC data extracted from a circular central region (*lower panel*) and a rectangular region along the southern ridge of CTA 1 (see Fig. 1). The power-law component is dominant in the central region, while the thermal component comprises 50% of the flux in the ridge region. Similar results are observed from *ASCA* data, although only the central region was mapped (see text).

tistically improved with the addition of a soft thermal component ($kT = 0.21 \pm 0.03$ keV), which contributes ~25% of the unabsorbed 0.5–10 keV flux (~10% of the observed flux). The spectrum from the chip placed directly south of the bright center is similar to the above, but the thermal component is stronger (~40% of the unabsorbed flux). The power-law index is 2.3 ± 0.1, suggesting a softening of the emission with increasing radius.

Dividing the GIS spectra into two regions—a central circle of radius 9′.2 and a surrounding annulus of thickness 9′.2—confirms the expected increase in the contribution of the thermal component at larger radii by a factor of ~2. The relative flux values for these regions, assuming the best-fit spectral values described above, are listed in Table 1.

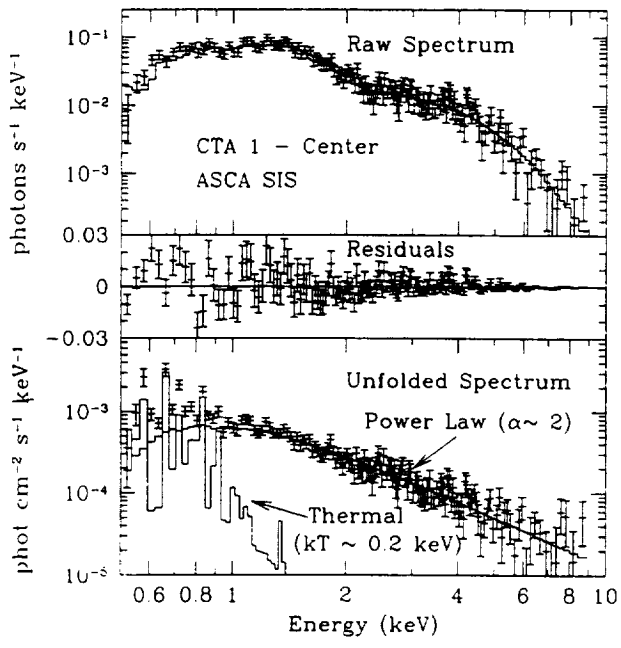

FIG. 4.—*ASCA* data extracted from a SIS chip centered on the central region of CTA 1 (see Fig. 1). *Upper panel*: Raw spectrum with best-fit power-law plus thermal model. *Middle panel*: Residuals between data and best-fit model. *Lower panel*: Unfolded spectrum and model components. Compare with predictions based upon PSPC spectra (Fig. 2—note that PSPC central spectral region does not cover the same angular size as the SIS chip).

3.2. *Timing*

A search for pulsations associated with a central pulsar was carried out using the GIS data. Using both high and medium bit rate data, we extracted all events from a circle 1′.5 in radius centered on the peak of the X-ray emission. A total of 408 (477) events were obtained from GIS2 (GIS3). No significant pulsations were detected in a 2^{23} point fast Fourier transform covering frequencies up to 50 Hz. From empirical results for measurements of pulsed fraction for detected pulsars, we derived an upper limit of ~45% for the pulsed fraction from the entire selected emission region.

If we assume a power-law index $\alpha = 1.5$ (similar to the Crab pulsar) for the point source discussed above, the expected number of counts contributed from this source is 270. This leads to an upper limit of 75% for the pulsed fraction from this source.

Since some pulsars show an increased pulsed fraction at higher energies (Ögelman & Finley 1993), we repeated the above analysis using only events with energies above ~2 keV. Again no significant pulsations were detected.

4. EMISSION CHARACTERISTICS

4.1. *Thermal Emission*

While the present *ASCA* observation confirms the non-thermal nature of the central emission from CTA 1, the limited angular coverage does not permit an accurate determination of the total luminosity of this emission component. Further, although the presence of a soft, probably thermal, component to the remnant emission has also been confirmed, the current *ASCA* coverage is insufficient to determine the associated emission measure over the entire remnant. As a plausible (if unproved) scenario, we consider the case of a remnant in the Sedov phase of evolution (Sedov 1959) accompanied by a strong synchrotron nebula driven by a central pulsar. Assuming a shell-type geometry for the thermal component, we may scale the thermal emission measure derived from the central region (a small fraction of the shell in projection) to provide an approximation to that of the entire remnant.

The normalization from the spectral fit is $K = \mathrm{EM}/(4\pi D^2)$, where $\mathrm{EM} = \int n_H n_e dV$ is the volume emission measure and D is the source distance. Averaging the results from the two GIS detectors, we measure $K = (1.1^{+1.1}_{-0.5}) \times 10^{13}$ cm^{-5} for the portion of the remnant observed. The Sedov solution provides the radial density distribution from which the volume emission measure can be derived. We integrate this distribution over the observed portion of the remnant in order to calculate an expected value for the spectral fit normalization. Assuming cosmic abundances, this leads to a preshock hydrogen density $n_0 = 3.7 \times 10^{-2} D_{1.4}^{-1/2}$ cm^{-3}, where $D_{1.4}$ is the remnant distance in units of 1.4 kpc (Pineault et al. 1993). The factor of ~2

uncertainty in the spectral fit normalization leads to ~40% uncertainty in n_0.

Assuming the soft thermal component corresponds to the emission-measure–weighted temperature for a Sedov remnant (Table 1), the corresponding shock temperature is $T_s = 1.8 \times 10^6$ K. The remnant age is thus $t = 2.0 \times 10^4 D_{1.4}$ yr. This leads to an explosion energy $E_{SN} = 0.6 \times 10^{50} D_{1.4}^{5/2}$ ergs and a swept-up mass of $M_{sw} = 32.6 D_{1.4}^{5/2} M_\odot$.

The derived value for n_0 is quite small, but not unrealistic for the location of CTA 1 at $250 D_{1.4}$ pc above the Galactic plane; average $n(z)$ models (e.g., Dickey & Lockman 1990) suggest values $\lesssim 0.1$ cm^{-3} at this height.

The somewhat low explosion energy could be reconciled with the more typical values of ~ 0.5–1×10^{51} ergs if the distance has been underestimated by a factor of ~3, although this would decrease the already low calculated value of n_0 by a factor of ~1.7. The kinematic distance of 1.4 ± 0.3 kpc (Pineault et al. 1993) is based upon a presumed association between the SNR and a shell of H I emission at velocity between -12 and -20 km s^{-1}. If this association is indeed correct, it would appear difficult to derive an explosion energy considerably larger than 10^{50} ergs. We note, however, that the values derived above are based upon the assumption that the observed electron temperature is representative of the shock temperature. If the electrons and ions have not yet reached temperature equilibrium, then the shock temperature will be larger than assumed. For a remnant as evolved as CTA 1, Coulomb equilibration alone is sufficient to limit the ion/electron temperature ratio to values $\lesssim 2$. At most, therefore, the age could be reduced by ~50% and the resulting explosion energy could increase by a factor of ~2.

4.2. *Nonthermal Emission*

The total flux attributable to the nonthermal emission component observed within the central 18′.5 of the GIS field of view is $F_X(0.5\text{–}10 \text{ keV}) \approx 2.4 \times 10^{-11}$ ergs cm^{-2} s^{-1}. The associated luminosity is $L_X = 5.6 \times 10^{33} D_{1.4}^2$ ergs s^{-1}. We note that this is a factor of ~2.8 smaller than the flux quoted in SSS95 (when the latter is extrapolated to the 0.5–10 keV bandpass). This is the result of a better determination of the spectral index leading to a harder spectrum than previously calculated. If we model the nonthermal spectral component as uniformly filling a spherical volume of uniform density, then the ratio of the flux obtained from a 9′.2 circular region (9×10^{-12} ergs cm^{-2} s^{-1}) to that above implies a radius $R_p = 17'.7 = 7.2 D_{1.4}$ pc. While in principle the X-ray size may be smaller that the actual size of the plerion, we take R_p to be coincident with the actual radius of the plerion; this also implies that the GIS field of view collects the whole nonthermal flux. We note, however, that PSPC spectral results suggest extension of the nonthermal component beyond this central region. Further spectral studies of the outer remnant regions, at higher resolution, are required to further address this issue.

The presence of a dominant power-law component in the central spectrum of CTA 1 clearly suggests the presence of a central pulsar. We note that source 7 (subsequently identified as J000702+7302.9 in the WGACAT; White, Giommi, & Angelini 1997) from the list of unresolved sources within CTA 1 compiled by SSS95 is located at the position of the peak diffuse X-ray emission seen in Figure 1. Assuming a power-law spectrum with photon index of 1.5 for this source, similar to that of the Crab pulsar, the 0.1–2.4 keV flux is 1.8×10^{-13} ergs cm^{-2} s^{-1} (2.5×10^{-4} photons cm^{-2} s^{-1}), leading to an X-ray luminosity of 4.3×10^{31} ergs s^{-1} at a distance of 1.4 kpc, typical of moderate-aged pulsars. The luminosity ratio between this source and that for the extended synchrotron component would be ~0.8%, quite low compared with other pulsar/synchrotron nebula associations.

There also exists an unidentified EGRET source whose position is consistent with the point source at the center of CTA 1. Nolan et al. (1996) identify J0009+73 as a high-energy γ-ray source with a measured flux of $F_\gamma(>100 \text{ MeV}) = (55.5 \pm 8.0) \times 10^{-8}$ photons cm^{-2} s^{-1}. The photon index for the source is 1.58 ± 0.20. Extrapolation of this spectrum back to the *ROSAT* band (0.1–2.4 keV) yields a predicted flux equal to that observed for the point source, if we assume a photon index of 1.41. Alternatively, extrapolation of the plerion flux to the EGRET band (using the observed spectral index of 2.03) predicts a flux which is more than a factor of 10 smaller than the observed EGRET flux. While the nonthermal flux measured with *ASCA* must be considered a lower limit (in that the emission may persist outside the observed region), an increase by such a large factor is inconsistent with strict geometric scaling to the full size of CTA 1. Further, both the *ROSAT* and the *ASCA* data indicate that the strength of the nonthermal component decreases toward the periphery. Finally, a spectral index of 2.03 is inconsistent with the quoted index for the EGRET source; for the plerionic emission to extend from the *ASCA* band to the EGRET band would require a spectral break with a decrease in the spectral index, which seems unlikely. We thus conclude that the EGRET emission is more likely to be associated with the point source.

Such an association also presents difficulties. If the source is indeed a pulsar, then there should be a significant cooling component to the X-ray emission. Indeed, the observed flux is consistent with that expected from standard cooling models, thus leaving little to associate with magnetospheric emission. The EGRET data also indicate that the source is variable at about the 2.2 σ confidence level. Such variability, if real, would be problematic for the association of J0009+73 with a pulsar. We note that the AGN discussed in § 1 is just outside the position error box by Nolan et al. (1996). An association with this source would be consistent with variability.

5. DISCUSSION

The nonthermal emission from CTA 1 is presumably associated with a plerion driven by a central pulsar. We may use the derived thermal and nonthermal characteristics of the remnant to investigate the evolutionary properties of the pulsar and its plerion.

From the luminosity of the nonthermal component described above, the current spin-down energy loss rate of the pulsar, $\dot{E}$, can be derived using the empirical relationship $\log L_X = 1.39 \log \dot{E} - 16.6$ derived by Seward & Wang (1988). Thus, $\dot{E} = 1.7 \times 10^{36} D_{1.4}^{1.4}$ ergs s^{-1}. Using this along with the SNR age derived from the Sedov analysis, we may derive the current spin period (Seward & Wang 1988),

$$P \approx \frac{1.4 \times 10^{23}}{(\dot{E}t)^{1/2}} \approx 0.14 D_{1.4}^{-1.2} \text{ s} ,$$

and the spin-down rate,

$$\dot{P} = \frac{P}{2t} = 1.1 \times 10^{-13} D_{1.4}^{-2.2} \text{ s s}^{-1} .$$

Further, a lower limit for the initial spin period, P_0, is established by the condition that the initial spin energy of the pulsar was less than the thermal energy derived from the Sedov analysis. To see this, consider an initial pulsar spin energy in excess of the blast wave energy; as the pulsar evolves, the energy contributed in the form of magnetic flux would drive the SNR evolution and increase the thermal energy unless the initial pulsar energy loss was strongly imbalanced in favor of particle acceleration (which seems unlikely). Thus, $P_0 > 1.2 \times 10^{-2} D_{1.4}^{-5/4}$ s.

For the magnetic dipole model, we can write

$$\dot{E}\tau^2 = \frac{3I^2c^3}{8a^6B_\perp^2} \approx 10^{61} B_{12}^{-2} \text{ ergs s}^{-1} ,$$

where $a \approx 10^6$ cm is the neutron star radius, I is the moment of inertia, B_{12} is the surface magnetic field at the equator in units of 10^{12} G, and $\tau = P/(2\dot{P})$ is the pulsar characteristic age. Using the above, we find $B_{12} = 3.9 D_{1.4}^{-1.7}$.

We next consider the plerion evolution. The Sedov solution discussed in Section 4.1 leads to a central thermal pressure $P_c = 2.6 \times 10^{-11} D_{1.4}^{-1/2}$ dynes cm^{-2}. The derived age of the remnant is sufficiently large for the reverse shock to have passed the plerion boundary, thus leaving the plerion magnetic pressure in equilibrium with the ambient thermal pressure (Reynolds & Chevalier 1984). This leads to a nebular magnetic field $B = 25 D_{1.4}^{-1/4}$ μG. Assuming a power-law spectrum for electrons injected into the nebula of size $R_p = 17'.7$ (see above), standard synchrotron theory (e.g., Ginzburg & Syrovatskii 1965) yields an energy density $U_e = 3.0 \times 10^{-16} B_{-4}^{-3/2} D_{1.4}^{-1}$ ergs cm^{-3} for the electrons producing the X-ray emission, where B_{-4} is the field strength in units of 10^{-4} G. Using the above field, we find $U_e = 2.4 \times 10^{-15} D_{1.4}^{5/8}$ ergs cm^{-3}. The current magnetic energy density is thus roughly 10,000 times larger than the energy density of the X-ray–emitting electrons. We note that this electron energy density is a lower limit since it corresponds only to those whose flux is produced in the X-ray band. If these electrons represent a large fraction of the total electron energy, this implies a large imbalance with the magnetic energy density at the present epoch. As we discuss below, such an imbalance is consistent with approximate equipartition between particle and magnetic flux input from the pulsar given the synchrotron losses experienced by the particles since injection (Bandiera, Pacini, & Salvati 1996).

If we define p as the fraction of the pulsar spin-down power which appears as magnetic flux injected into the nebula, then we may write

$$\frac{d}{dt}\left(\frac{B^2R_p^4}{6}\right) = p\dot{E}R_p .$$

For magnetic dipole losses from a pulsar, we have

$$\frac{\dot{E}}{\dot{E}_0} = \left(1 + \frac{t}{\tau_0}\right)^{-2} .$$

Let us assume that at times smaller than τ_0 the plerion expansion was approximately linear (i.e., the Sedov phase begins at some later time t_S; see Reynolds & Chevalier 1984), with a typical expansion velocity v_0. Upon integrating to t_S, we find:

$$\frac{B^2R_p^4}{6} = pv_0(\dot{E}_0\tau_0^2)\left[\ln\left(1 + \frac{t_S}{\tau_0}\right) - \left(\frac{t_S}{t_S + \tau_0}\right)\right].$$

The quantity in brackets lies in the approximate range 1–3 for values of t_S/τ_0 in the range 5–50. Including evolution beyond t_S increases this quantity only slightly ($\sim$25%) since the bulk of the magnetic flux is injected from the pulsar at earlier times; we thus approximate this factor by 2. For times $t \gg \tau_0$, we have $\dot{E}t^2 \approx \dot{E}_0\tau_0^2$. Using the value of $\dot{E}$ from above, along with the age from the Sedov solution, we thus have

$$p \approx 0.21\left(\frac{v_0}{1000 \text{ km s}^{-1}}\right)^{-1} D_{1.4}^{0.1} .$$

Thus, for reasonable values of the expansion velocity ($v_0 \approx$ 1400 km s^{-1} for the Crab), we see that the particle and magnetic flux processes are roughly in equipartition at the time of injection. An exact equipartition is attained if the plerion radius has been underestimated by $\sim$25%.

6. CONCLUSIONS

We have used new observations of CTA 1 carried out with the *ASCA* X-ray observatory to establish the nonthermal nature of the central emission. The observed characteristics are consistent with a synchrotron nebula powered by a central pulsar. The point source J000702+7302.9 resides at the center of the diffuse synchrotron emission and represents a viable candidate for the pulsar based upon position and X-ray luminosity. The possible association of this source with the unidentified γ-ray source J0009+73 adds further interest to more detailed investigations. In particular, high-resolution imaging of the source, with high time resolution, should be carried out to search for evidence of pulsations which would confirm the association. Similarly, a high-sensitivity radio search for evidence of an associated pulsar is of interest.

The *ASCA* observations also support the presence of a weak thermal component which may be associated with shock-heated gas from the ISM. If interpreted as emission from a Sedov phase remnant, CTA 1 appears to represent a curious case of an old remnant, with a Crab-like core, which was produced in a low-energy explosion high above the Galactic plane. Joint consideration of the thermal and nonthermal components suggests a pulsar with a spin period of $0.14 D_{1.4}^{-1.2}$ s and a surface magnetic field of $3.9 \times 10^{12} D_{1.4}^{-1.7}$ G. Pressure balance between the plerion and the thermal interior of the SNR yields a nebular magnetic field strength of $25 D_{1.4}^{-1/4}$ μG which implies a large imbalance between the magnetic and electron energy densities at the current epoch, but is consistent with equipartition at the time of injection.

The authors would like to thank Olaf Vancura, Jack Hughes, and Ilana Harrus for helpful discussions and suggestions for the text. K. T. is supported by Research Fellowships of the Japan Society for the Promotion of Science for Young Scientists. R. B. gratefully acknowledges the hospitality of the Smithsonian Astrophysical Observatory during the course of this work. This work was supported in part by the National Aeronautics and Space Administration through contract NAS 8-39073 and grants NAG 5-2638 and NAG 5-3486.

REFERENCES

Bandiera, R., Pacini, F., & Salvati, M. 1996, ApJ, 465, L39
Dickey, J. M., & Lockman, F. J. 1990, ARA&A, 28, 215
Ginzburg, V. L., & Syrovatskii, S. I. 1965, ARA&A, 3, 297
Harrus, I. M., Hughest, J. P., Singh, K. P., Koyama, K., & Asaoka, I. 1997, ApJ, submitted
Nolan, P. L., et al. 1996, ApJ, 459, 100
Ögelman, H., & Finley, J. P. 1993, ApJ, 413, L31
Pineault, S., Landecker, T. L., Madore, B., & Gaumont-Guay, S. 1993, AJ, 105, 3, 1060
Pineault, S., Landecker, T. L., Swerdlyk, C. M., & Reich, W. 1997, A&A, in press
Raymond, J. C., & Smith, B. W. 1977, ApJS, 35, 419
Reynolds, S. P., & Chevalier, R. A. 1984, ApJ, 278, 630
Rho, J.-H., Petre, R., Schlegel, E. M., & Hester, J. J. 1994, ApJ, 430, 757
Sedov, L. 1959, Similarity and Dimensional Methods in Mechanics (New York: Academic)
Seward, F. D., Schmidt, B., & Slane, P. 1995, ApJ, 453, 284
Seward, F. D., & Wang, Z-R. 1988, ApJ, 332, 199
Smith, A., Jones, L. R., Peacock, A., & Pye, J. P. 1985, ApJ, 296, 469
Torii, K., Tsunemi, H., Kinugasa, K., & Slane, P. 1997 in X-ray Imaging and Spectroscopy of Cosmic Hot Plasmas, ed. F. Makino & H. Mitsudo (Tokyo: Universal Academy), 395
Yamauchi, S., Kaneda, H., Koyama, K., Makishima, K., Matsuzaki, K., Sonobe, T., Tanaka, Y., & Yamasaki, N. 1996, PASJ, 48, L15
White, N. E., Giommi, P., & Angelini, L. 1997, in preparation

Minnesota Astronomy Centennial
10^{51} Ergs: The Evolution of Shell SNRs
Poster Session

Session 1: Very Young Remnants

1.01

Laboratory Simulation of Hydrodynamic Phenomena in Supernova Remnants

R. Paul Drake (U. Michigan), S. Gail Glendinning (Lawrence Livermore National Lab), Kent Estabrook (LLNL), Richard McCray (U. Colorado), Bruce Remington (LLNL), A.M. Rubenchik (U.C. Davis), E. Liang (Rice) R. London (LLNL), R.J. Wallace (LLNL), J. Kane (U. Arizona)

We are developing experiments[1] using the Nova laser to investigate hydrodynamic phenomena relevant to supernova explosions[2] and to SNRs. Our aim is to provide tests of the computational models now used to interpret the astrophysical observations, and also to provide data that suggests directions for their improvement. In experiments relevant to Very Young SNRs, we are investigating the evolution of the hydrodynamic assembly formed by the collision of high-Mach-number ejecta with ambient plasma. This is motivated by modeling of SN1987A. The aim is to improve the predictions of the impending collision between such an assembly and the nebular ring. Further experiments will produce radiative hydrodynamic systems. These will be relevant to remnant formation in the more typical Type II SN having a denser circumstellar medium. The SNR experiments and their connections to modeling will be discussed. (Work supported by the US Department of Energy.) [1] B.A. Remington et al., in press, Phys. Plasmas (May, 1997) [2] J. Kane et al., in press, Ap. J. Lett. (March-April, 1997).

1.02

The Nature of Recent Radio Supernovae

Schuyler D. Van Dyk (Visiting scientist at UCLA), Marcos J. Montes (NRC/NRL), Richard A. Sramek (NRAO/VLA), Kurt W. Weiler (NRL), Nino Panagia (ESA/STScI)

The radio emission from supernovae (SNe) is nonthermal synchrotron radiation of high brightness temperature, with a "turn-on" delay at longer wavelengths, power-law decline after maximum with index β, and spectral index α asymptotically decreasing with time to a final, optically thin value. Radio supernovae (RSNe) are best described by the Chevalier (1982) "mini-shell" model,with modifications by Weiler et al. (1990). RSNe observations provide a valuable probe of the SN circumstellar environment and progenitor system. We present a progress report on the nature of the recent Type IIb SNe 1993J and 1996cb, and of the Type Ic SN 1994I.

1.03

Radio Emission from Supernovae

S.D. Van Dyk (UCLA), M.J. Montes (NRC/NRL), K.W. Weiler (NRL), R.A. Sramek (NRAO-VLA), N. Panagia (STScI/ESA), R. Park (TJHS)

Radio supernovae (RSNe) are an excellent means of probing the circumstellar matter around, and therefore the winds from, supernova (SN) progenitor stars or stellar systems. The observed radio synchrotron emission is best described by a modified Chevalier model which involves the generation of relativistic electrons and enhanced magnetic field through the SN shock interacting with a relatively high-density circumstellar envelope, presumed to have been established through mass loss in the late stages of stellar evolution.

Since the detection of SN 1979C in 1980, extensive data have been collected and analyzed for two dozen RSNe.

variety of

loss times, and a power law spectrum with a spectral index of alpha = 1.3 +- 0.2, we conclude that the hard X-ray feature is synchrotron radiation from a site of enhanced particle acceleration. Evidence against a plerion includes a lack of observed periodicity (the pulsed fraction upper limit is 33spectral similarity with another more extended hard region, the location of the source outside the 95source, the fact that it is nestled in a bend in the molecular cloud ring with which IC 443 is interacting, and the requirement of an extremely high transverse velocity (¿ 5,000 km/s). We conclude that the anomalous feature is most likely tracing enhanced particle acceleration by shocks that are formed as the supernova blast wave impacts the ring of molecular clouds.

4.19

A ROSAT Study of Centrally-Condensed X-ray Supernova Remnants

Knox S. Long (STScI), Willaim P. Blair (JHU), P. Frank Winkler (Middlebury College)

The ROSAT PSPC has been used to observe four supernova remnants, HB 3, HB 9, HB 21, and W 63, that are members of the class of remnants with shell-like radio and/or optical morphologies and centrally condensed X-ray morphologies. The ROSAT X-ray images of all of the SNRs show considerable internal structure. In the cases of HB 3 and HB 9 the X-ray emission almost fills the region within the radio shell. The emission from HB 21 and W 63 does not fill the radio shell, but this may simply be due to the fact that these two SNRs are fainter and the surface brightness of the outer portions of the SNRs falls below our surface brightness limit.

The ROSAT spectra of all four remnants are similar, peaking sharply at about 0.9 keV, and arise most likely from thermal X-ray emission from normal abundance plasmas with effective temperatures in the range 0.2 - 0.7 keV. The X-ray observations are supplemented by new HA and [S II] images obtained for this study. In general, there is a poor correlation between the X-ray and radio or optical structures in these SNRs. The thermal energy content of the hot gas we detect in HB3 and HB9 is close to that expected of a typical SN explosion, but the energy content of the hot gas in HB21 and W63 is far less, consistent with the suggestion that these two SNRs are well into the radiative phase of their evolution.

Session 5: Thermal-Filled Composite Remnants

5.01

ASCA Observations of Two Composite SNRs: VRO42.05.01 and 3C400.2

David Burrows (Penn State U.), Zhiyu Guo (Goddard Space Flight Center)

We present ASCA observations of two old composite SNRs: VRO42.05.01 and 3C400.2. Both remnants have a center-filled X-ray morphology which has been interpreted on the basis of ROSAT PSPC data as consistent with the White and Long model of evaporation of embedded cloudlets. The X-ray spectra of the two differ dramatically. VRO42.05.01 has a nearly featureless spectrum, consistent with very low abundances of Mg and Si. 3C400.2 has strong Si and Mg lines. We discuss our spectral fitting results and possible explanations for the spectral differences.

5.02

Center-Filled X-ray Morphology in SNRs

Patrick Slane (Harvard-Smithsonian Center for Astrophysics), J.P. Hughes (Rutgers), R. Petre (NASA/GSFC), J.-H. Rho (Saclay)

A distinct subset of moderate age remnants are characterized by an X-ray morphology which is centrally brightened, in complete contrast to the limb-brightened radio profile. In some cases (e.g. CTA 1, MSH 11-62), recent observations have shown that the central emission is nonthermal in nature, presumably associated with a pulsar-driven synchrotron nebula. For others, however, the central emission is decidedly thermal. The evolutionary characteristics which have led to such an observed profile are not well understood. One possible scenario is that the

shells in these remnants have recently gone radiative, thus leaving only the hot interior to persist in X-rays. Another suggestion is that the central emission measure has been enhanced by the presence of cool clouds left relatively intact after the passage of the blast wave to slowly evaporate in the hot remnant interior. We have applied models for these scenarios to the X-ray brightness and temperature profiles for the center-filled SNRs MSH 11-61A and W28. Here we report on the results of this study and discuss the age, energy, and density characteristics implied by the models for these remnants.

5.03

Excitation and disruption of a molecular cloud by the 3C391 supernova remnant

Rho, J.-H. (CEA-Saclay, France) and Reach, W. T. (IAS-Orsay, France)

The interactions with clouds, which possibly provide evaporating clouds, are being confirmed in infrared and millimeter wavelengthes for 3C391 and W44. The brightness of the [OI] 63 μm line, an energy tracer, was $\sim 0.3 - 1.4 \times 10^{-3}$ erg cm^{-2} sr^{-1}, detected in the 20 positions observed toward both remnants. The lines of 3C391 and W44 are brightest strongly peaked, at the edges of the remnants, which brightness suggest pre-shock densities $> 10^3$ cm^{-3} and ram pressures of order 10^{-7} dyne cm^{-2}, compared with theoretical models (e.g. Hollenbach & Mckee 1989), as might occur for a supernova blast wave interacting with a molecular cloud. Continuum emission toward the remnant, expected from dust heated by the shock is detected. The radiative energy loss infers that the remnants are in Sedov Stage, rather than a radiative phase. We have also mapped a molecular cloud, into which the shock front of the SNR 3C391 is currently impacting, in three lines of CS simultaneously, HCO+ and 12CO (J=2-1) using IRAM 30m telescope, in order to study the excitation of molecular gas by a fast shock. We detected a broad wing in all CS lines as well as in HCO+, which are as broad as that of the only other clear example of molecular shock in IC443. With our map of the CS line ratio, we will present if there are pre-existing dense condensations in the pre-shock cloud, which survive the initial blast wave and evaporate inside the remnant, and if it can explain the center-filled X-ray emission.

5.04

ASCA Observations of MSH15-56

Paul Plucinsky (Smithsonian Astrophysical Observatory)

We present ASCA observations of the SNR MSH15-56. MSH15-56 is an example of a remnant which defies classification schemes; it is a "composite" SNR in the radio and has a complex X-ray morphology consisting of a partial shell and a bright, central enhancement. The remnant has the classic composite morphology in the radio consisting of a compact central region with a non-thermal spectrum with alpha= -0.1 and an outer shell, also with a non-thermal spectrum but with a significantly steeper spectrum, alpha = -0.4. The X-ray enhancements are not spatially coincident with the central radio enhancement; but they curiously lie on either side of the radio enhancement. The ASCA data show that the X-ray emission from the central region is completely thermal, while the emission from the SW shell is a mixture of thermal and non-thermal components, with the non-thermal component accounting for about 20 GIS spectrum from the central region is well-fitted by an equilibrium, Raymond-Smith model with solar abundances and the spectrum from the SW shell is well-fitted by an equilibrium, Raymond-Smith and a power-law model. There is some evidence for an overabundance of Si in the central region. We will discuss possible explanations for the existence of the non-thermal component in the SW shell and also compare the ASCA data with the ROSAT data to better determine the overall structure and evolutionary state of the remnant.

5.05

Study of the Composite Remnant MSH 11-62

Harrus (Harvard-Smithsonian Center for Astrophysics), Dr. John Hughes (Rutgers U.), Dr. Patrick Slane (Harvard-Smithsonian Center for Astrophysics)

We present an analysis of the X-ray data collected during an observation of the supernova remnant (SNR) MSH 11-62 by the *Advanced Satellite for Cosmology and Astrophysics* (ASCA). We show that MSH 11-62 is a composite

remnant whose X-ray emission comes from two distinct contributions: a nonthermal, synchrotron emission, dominating the total flux above 2 keV, and localized to a region of radius 3' (consistent with a point source) and a thermal component, extended up to a radius of 5' and detected only at energies below 2 keV. The spatial and spectral analysis imply, in the context of empirical models, the presence of a neutron star, losing energy at a rate of about dE/dt .2 10^{36} ergs s^{-1}. The period of the neutron star is estimated to be around 0.380 sec although our timing analysis leads to only an upper limit to the pulsed fraction of 10This is consistent with the lack of a radio pulsar in the remnant, which may be due to insufficient sensitivity of published searches or may indicate that the pulsed emission from the rapidly rotating compact object that should be powering the synchrotron nebula is beamed and our viewing direction is unfavorable. In either event, the central neutron star deposits much of its spin-down energy into the surrounding synchrotron nebula where, through direct imaging with broadband satellites such as ASCA, it is possible to study the energetics and evolution of the compact remnant.

5.06

The Case for Thermal Conduction in Thermal Composite-Type Supernova Remnants

R. L. Shelton (NASA/Goddard Space Flight Center), D. P. Cox (Dept. of Physics, U. Wisconsin – Madison), R. K. Smith (NASA/Goddard Space Flight Center), W. Maciejewski (Dept. of Astronomy, U. Wisconsin – Madison), T. Plewa (Max Planck Institute for Astrophysics), R. Petre (NASA/Goddard Space Flight Center), A. Pawl (Dept. of Physics, U. Wisconsin – Madison)

Thermal conduction within the interior of a supernova remnant bubble acts to transport energy away from the very hot center. While the central temperature is much lower than in a Sedov model, the central pressure is little affected. Consequently, the central density is much larger than in the Sedov model. These conditions dramaticly increase the central X-ray luminosity over that found without thermal conduction and may explain the thermal X-ray bright centers found in some thermal composite supernova remnants. We compare computer model results and observations for supernova remnant W44 and comment on other remnants.

5.07

The Radio Spectral Index of the Crab Nebula

Namir E. Kassim (Naval Research Laboratory), M.F. Bietenholz (York U.), D.A. Frail (NRAO), R.A. Perley (NRAO)

We present the results of a new, comprehensive investigation of the radio spectral index of the Crab Nebula supernova remnant. New data at 74 MHz is combined with data at 327 MHz, 1.5 GHz and 5 GHz. In contrast to previous claims, little spatial variation in the spectral index is seen. In particular, between 327 MHz and 5 GHz we see no evidence of spectral steepening near the edge of the nebula, the "jet" or the ionized filaments. The rms limits on any spectral index variations in these regions amount to no more than 0.01. We believe that earlier reports of large steepening were the result of correlator bias or registration problems. An elongated feature was detected 1 arcmin northwest of the pulsar which is probably due to a moving feature rather than an actual spectral index anomaly. It may be related to the well-known wisp-like structures seen closer to the center of the nebula. At 74 MHz, we see for the first time, evidence of free-free absorption by the thermal material in the Crab Nebula's filaments. Apart from some possible renewed acceleration occurring in the wisps, the dominant accelerator of relativistic electrons in the Crab nebula is the pulsar itself.

Session 6: Pulsar-Powered Remnants

6.01

The Shock at the Outer Boundary of the Crab Nebula

Ravi Sankrit (Arizona State U.), J Jeff Hester (Arizona State U.)